ELSEVIER

Journal of Molecular Structure: THEOCHEM 771 (2006) 129–133

THEO CHEM

www.elsevier.com/locate/theochem

Structure of small Au_n, Ag_n, and Cu_n clusters ($n=2-4$) on rutile $TiO_2(110)$: A density functional theory study

Devina Pillay, Gyeong S. Hwang *

Department of Chemical Engineering, The University of Texas at Austin, Austin, Texas 78712

Available online 21 April 2006

Abstract

We examine the structure of small Au_n, Ag_n, and Cu_n ($n=2-4$) clusters on rutile $TiO_2(110)$ surfaces using density functional theory calculations. Based on the comparison of supported and gas-phase clusters, we also discuss the effect of the cluster–substrate interaction on the atomic structure of small Au, Ag, and Cu clusters grown on $TiO_2(110)$.

Keywords: Density functional theory calculations; growth; metal; metal-oxide; gold; silver; copper; titantium dioxide

1. Introduction

Oxide supported noble metal nanoclusters often exhibit higher activity than their bulk counterparts [1,2]. Their catalytic activities have been found to depend markedly on the cluster size, shape, and size distribution, which are largely determined by the surface properties of the supporting oxide [3–5]. Despite long lasting efforts little is known about the role of cluster–support interactions in the growth, structure, and reactivity of supported metal catalysts [6]. This is due in large part to difficulties in direct characterization of buried cluster–support interfaces [3].

Over recent years significant advances in computing power and theoretical methods have made it possible to explore the structure and reactivity of oxide-supported metal clusters using first principles quantum mechanical calculations. Such first principles studies allow an accurate assessment of the nature of cluster–support interfacial interactions. This will in turn greatly assist in not only understanding the growth mechanism of metal clusters, but also revealing the fundamental processes behind their unusual catalytic properties.

In this paper, we present structural models for small Au_n, Ag_n, and Cu_n clusters ($n=2-4$) on rutile $TiO_2(110)$ and their relative stability based on extensive density functional theory (DFT) calculations. Previous theoretical studies [7,8] reveal that the nucleation of Au clusters predominantly occurs at oxygen vacancy sites, whereas Ag and Cu clusters interact more strongly with bridging oxygen atoms than oxygen vacancies. Thus, in this study we only examine Au clusters at the vicinity of an oxygen vacancy on the reduced surface and Ag and Cu clusters on the stoichiometric surface. The titania-supported 1B metals clusters not only show distinctly different growth modes and sintering behaviors, but also altering catalytic properties [9]. Recent experimental work for instance shows that small Cu and Ag clusters preferably evolve into three-dimensional (3D) structures at the initial stage of growth [10,11], while Au clusters for low coverage (<0.1 ML) show a 2D like growth, and then transitions to (3D) like growth mode when coverage exceeds 0.1 ML [12]. The present comparative study may provide some insight into such distinctions between 1B metal clusters dispersed on TiO_2.

2. Computational approach

All our calculations are performed based on spin polarized DFT within the generalized gradient approximation (PW91) [13] using planewave basis sets and ultrasoft pseudopotentials [14], as implemented in the Vienna ab initio simulation package (VASP) [15]. A plane-wave cut-off energy of 300 eV is used. The atomic structures are calculated using a 15 atomic-layer (2×3) slab that is separated from its periodic images by a vacuum space of 10 Å. Au atoms and all surface atoms in the top nine layers are fully relaxed using the conjugate gradient method until residual forces on the flexible atoms become smaller than 5×10^{-2} eV/Å. For the Brillouin Zone integration, we use a ($2\times4\times1$) Monkhorst–Pack mesh of k points for a (2×3) surface cell.

* Corresponding author. Tel.: +1 512 471 5238; fax: +1 512 471 7060.
E-mail address: sgshwang@che.utexas.edu (G.S. Hwang).

0166-1280/$ - see front matter © 2006 Published by Elsevier B.V.
doi:10.1016/j.theochem.2006.03.040

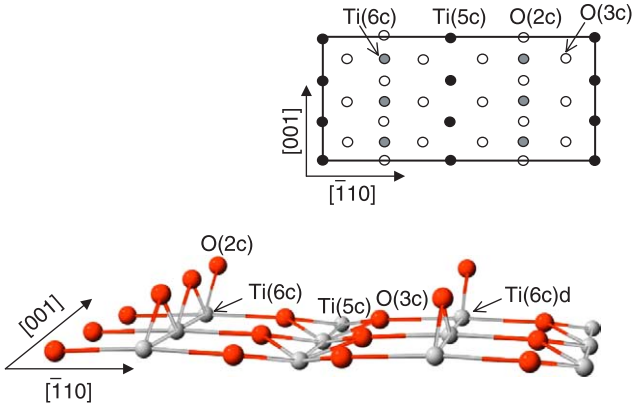

Fig. 1. Ball-and-stick representation of the stoichiometric TiO_2(110) surface. The red and grey balls represent O and Ti atoms, respectively. The inset shows the top view of the 2×3 surface cell. The white and black/grey balls represent O and Ti atoms, respectively (for interpretation of the reference to colour in this legend, the reader is referred to the web version of this article).

3. Results and discussion

3.1. TiO_2(110) rutile surface

As shown in Fig. 1, the stoichiometric TiO_2(110) surface consists of two types of Ti atoms and two types of O atoms: fivefold coordinate Ti(5c), sixfold coordinate Ti(6c) atoms, twofold coordinate (protruding) bridging oxygen O(2c), and threefold coordinate in plane O(3c) atoms. A reduced surface is prepared by removing a bridging O(2c) atom from a given surface cell. The Ti(6c) atoms initially bonded to the removed O(2c) atom become fivefold coordinated; [they are hereafter labeled as $Ti(6c)_d$]. Removal of a neutral bridging O(2c) atom results in two unpaired electrons that are greatly delocalized along the neighboring Ti(5c) rows [7,8,16]. This leads to a strong repulsive interaction between vacancies located adjacent to each other along the row [8]. As a result, the formation of vacancy pairs or larger vacancy clusters is energetically unfavorable, relative to isolated vacancies [7,8].

3.2. Gold clusters on reduced TiO_2(110)

Fig. 2 shows the optimized structures of a Au dimer, trimer, and tetramer. For the Au dimer, we consider the following configurations: (2-A) the dimer is aligned in the [001] direction between two bridging O(2c) atoms; (2-B) an Au atom is placed at the vacancy site, while the other Au atom interacts with an adjacent Ti(5c) atom; (2-C) the dimer is centered between two Ti(5c) atoms along the [001] direction; and (2-D) the dimer is placed vertically at the vacancy site. As summarized in Table 1, the structure shown in (2-A) turns out to be the most energetically favorable, followed by the structures shown in (2-B), (2-C), and (2-D). For the lowest-energy dimer [(2-A)], the bond length of 2.49 Å is slightly shorter than that of a neutral gas phase dimer, 2.54 Å [17], indicating that there is a geometric constraint from the titania surface. The dimer in (2-B) is predicted to undergo a transformation to the structure shown in (2-A), with a moderate barrier of 0.34 eV. This suggests the dimer in (2-B) would be an intermediate state for formation of the ground-state dimmer [(2-A)], via a sequence of diffusion and pairing of single Au atoms deposited on the

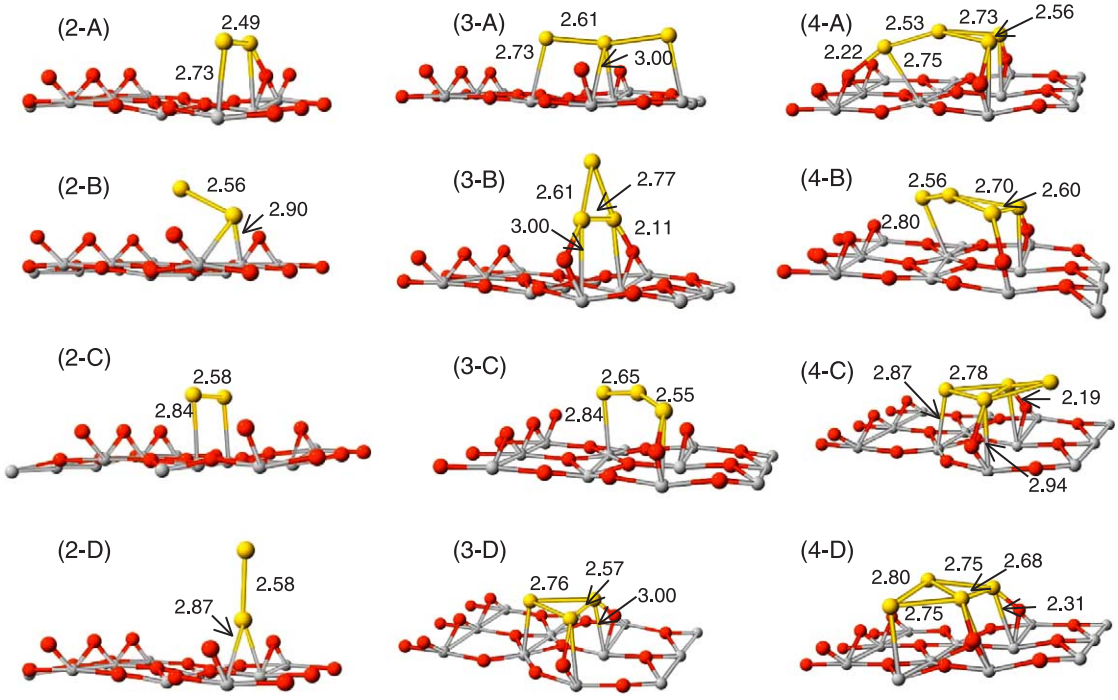

Fig. 2. Adsorption geometries of Au dimers, trimers, and tetramers on the reduced TiO_2(110) surface. Yellow, red, and grey balls represent Au, O, and Ti atoms, respectively. The bond lengths are given in angstrom. The corresponding adsorption energies are summarized in Table 1. The surface is modeled using a 15 atomic-layer slab. (for interpretation of the reference to colour in this legend, the reader is referred to the web version of this article).

Table 1
Calculated adsorption energies (eV) for Au clusters on the reduced TiO_2(110) rutile surface, as depicted in Fig. 1

	A	B	C	D
Au_2	1.36	0.65	0.52	0.46
Au_3	2.04	1.91	1.86	1.63
Au_4	1.90	1.53	0.99	0.95

surface. The structure in (2-D) can easily transform to the dimer shown in (2-B), and subsequently to the ground state structure, Fig. 2 (2-A). This suggests that the vertically aligned structure [(2-D)] is highly unlikely.

For the Au trimer, we consider following configurations: (3-A) a linear structure where the center Au atom is placed at the vacancy site and two end atoms interact with the Ti(5c) atoms; (3-B) an isosceles triangular structure, which is oriented along the [110] direction, where two bottom Au atoms are aligned in the [001] direction above the vacancy site; (3-C) a bent linear structure where an end Au atom is placed at the vacancy site, while the other end atom is located atop a neighboring Ti(5c) atom; and (3-D) a isosceles triangular structure in plane with the surface. The adsorption energies of these clusters are summarized in Table 1. From the 15 atomic-layer slab calculations, the linear structure (3-A) turns out to be energetically more favorable than the structures (3-B), (3-C), and (3-D) by 0.13, 0.18, and 0.41 eV, respectively. In the gas phase, the linear, isosceles triangle, and bent-linear states are, respectively favored for anionic, neutral, and cationic trimers [17,18]. On the reduced surface, the trimer is negatively charged by virtue of charge transfer from the vacancy, resulting in the stabilization of the Au_3 adsorption by the spin pairing effect [19].

For the Au tetramer, we consider four different configurations: (4-A) a 'Y-shaped' structure where the edge atom interacts with an O(2c) atom in the neighboring O(2c) row; (4-B) a skewed 'Y-shaped' structure where the edge atom interacts with a Ti(5c) atom in the neighboring Ti(5c) row; and (4-C) and (4-D) which are rhombus-type structures with different orientations. For the supported clusters, the 'Y-shaped' tetramers turn out to be far more favorable than the rhombus structures. In the gas phase, neutral and anionic Au tetramers prefer rhombus and Y-shaped structures, respectively [17,18]. We attribute the significant difference in stability between the Y-shaped and the rhombus structures to the strong cluster–substrate interaction, while possible charge transfer to the Au_4 particle from the surface could not be totally excluded. Note that, in the gas phase, neutral and anionic Au tetramers prefer rhombic and Y-type structures, respectively [17], while the Y-shaped configuration is only about 0.12 eV more stable than the rhombic one in the neutral state. We also believe that the strong particle–substrate interaction is responsible for the 2D growth of Au particles when the coverage is low [12].

3.3. Silver and copper clusters on stoichiometric TiO_2(110)

In Figs. 3 and 4, we present the optimized dimer, trimer, and tetramer structures of Ag and Cu, respectively.

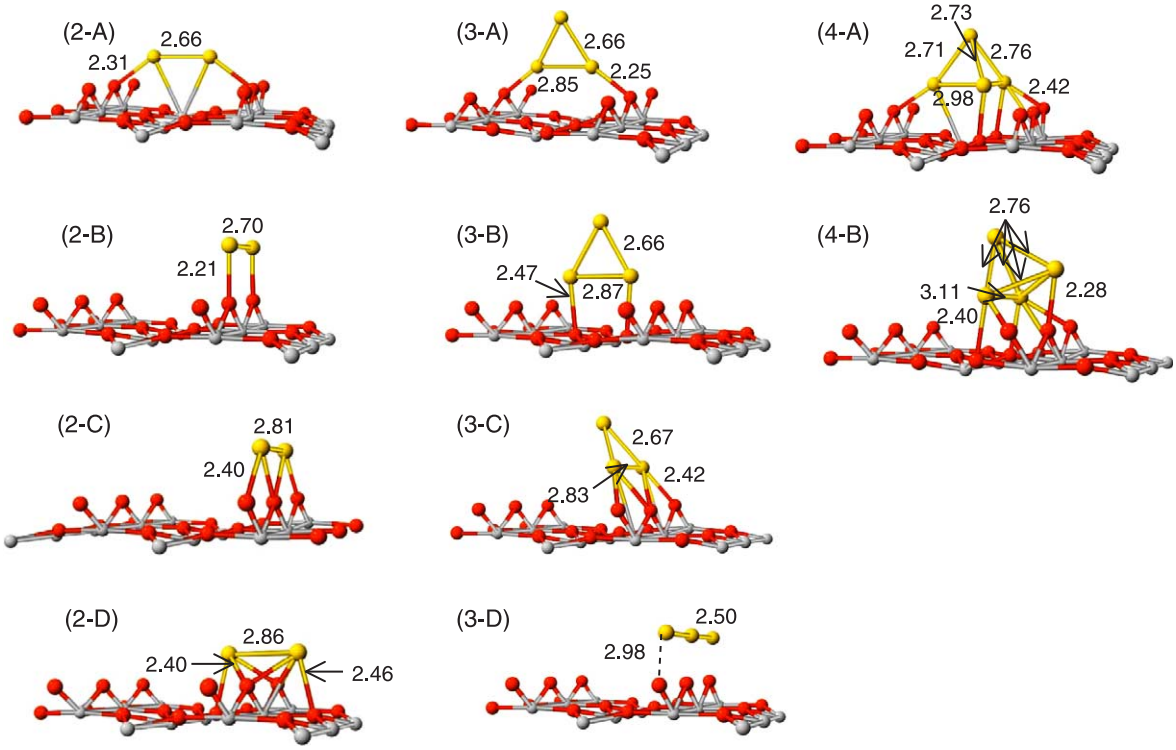

Fig. 3. Adsorption geometries of Ag dimers, trimers, and tetramers on the stoichiometric TiO_2(110) surface. Yellow, red, and grey balls represent Au, O, and Ti atoms, respectively. The bond lengths are given in angstrom. The corresponding adsorption energies are summarized in Table 2. The surface is modeled using a 15 atomic-layer slab. (for interpretation of the reference to colour in this legend, the reader is referred to the web version of this article).

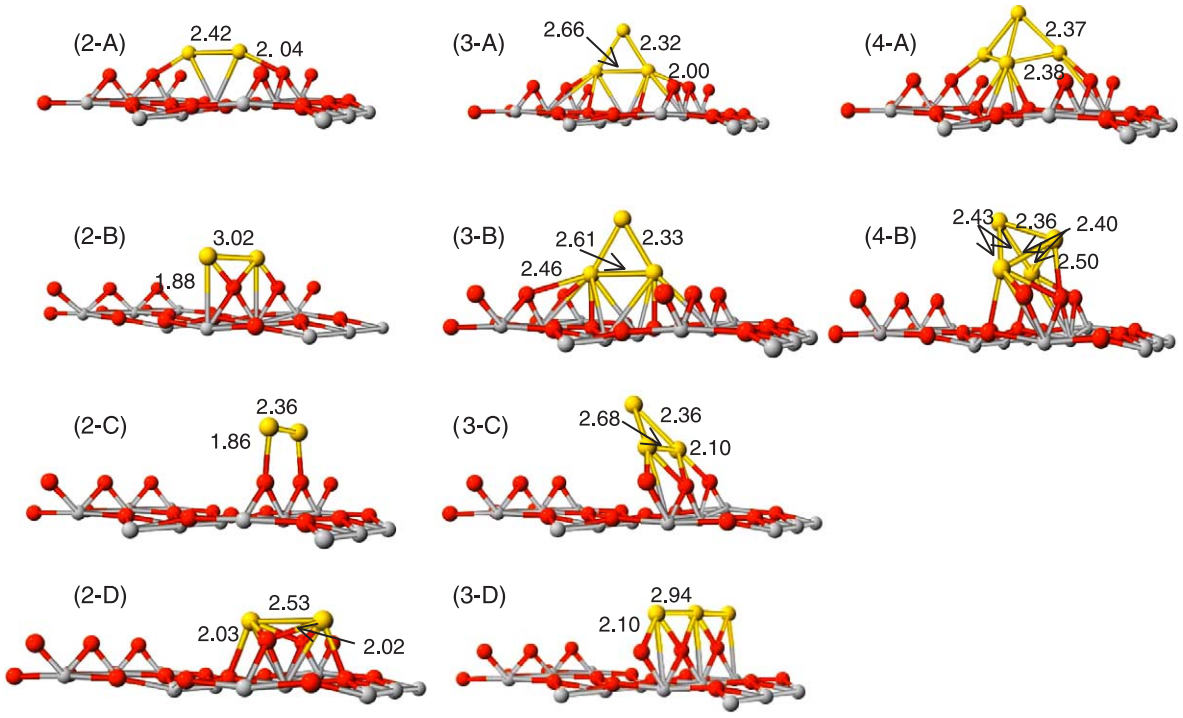

Fig. 4. Adsorption geometries of Cu dimers, trimers, and tetramers on the stoichiometric TiO_2(110) surface. Yellow, red, and grey balls represent Au, O, and Ti atoms, respectively. The bond lengths are given in angstroms. The corresponding adsorption energies are summarized in Table 3. The surface is modeled using a 15 atomic-layer slab. (For interpretation of the reference to colour in this legend, the reader is referred to the web version of this article).

The corresponding adsorption energies are summarized in Tables 2 and 3. These supported Ag and Cu clusters show similar atomic structures, as discussed below. We consider four stable configurations for Ag and Cu dimers on the stoichiometric TiO_2(110) surface: (2-A) the dimer is aligned between two bridging oxygen rows in the [-110] direction; (2-B)/(2-C) each Ag/Cu atom in the dimer is atop O(2c) atoms in the [001] direction; (2-C)/(2-B) each Ag/Cu atom in the dimer is in between O(2c) atoms along the [001] direction; and (2-D) the dimer is between two O(2c) atoms and is oriented along the [-110] direction. For all cases considered the bond length noticeably stretches compared to their neutral gas-phase counter parts (i.e. 2.57 Å for Ag_2 [20] and 2.42 Å for Cu_2 [21]). In the ground state structure [(2-A)], the shorter distance of 2.0 Å for Cu–O(2c) than 2.3 Å for Ag–O(2c) indicates Cu_2 interacts more strongly with the TiO_2 substrate than Ag_2. We also consider Ag and Cu dimers along the [001] direction above the Ti(5c) atoms, but they turn out to be far less favorable than the corresponding ground state structures [(2-A)]. This is not surprising because Ag and Cu clusters are stabilized largely by the electrostatic interaction with negatively charged O(2c) atoms [8].

As displayed in Figs. 3 and 4, we identify four stable configurations for supported Ag and Cu trimers: (3-A) an isosceles triangle which is centered upright over a Ti(5c) atom between two bridging oxygen rows in the [-110] direction; (3-B) an isosceles triangle which is centered above two in plane oxygen atoms; (3-C) an isosceles triangle which is oriented along the [001] direction above the bridging oxygen row; and (3-D) a linear configuration that is located above the bridging oxygen row along the [001] direction. The structures (3-A) and (3-B) are both centered along the [-110] direction, but the isosceles triangle [(3-A)] allows a stronger interaction between the Ag/Cu trimer and the O(2c) surface atoms. For the Ag/Cu case, this structure is predicted to be more energetically favorable than the other structures (3-B), (3-C), and (3-D) [as shown in Figs. 3 and 4] by 0.21/0.31 eV, 0.40/0.50 eV and 1.68/1.92 eV, respectively. The lowest-energy structure [(3-A)] of the supported Ag/Cu trimer has a C_{2v} symmetry, with a base length and base angle of 2.85 Å/2.66 Å and 58°/55°, respectively [21,22]. In the gas phase, for both Ag and Cu trimers the equilateral, isosceles triangle, and linear structures are, respectively favored for cationic, neutral, and anionic states [21–23]. Here, we expect there is charge transfer from

Table 2
Calculated adsorption energies (eV) for Ag clusters on the stoichiometric TiO_2(110) rutile surface, as depicted in Fig. 2

	A	B	C	D
Ag_2	1.17	0.59	0.69	0.58
Ag_3	2.71	2.50	2.31	0.54
Ag_4	3.08	2.37	–	–

Table 3
Calculated adsorption energies (eV) for Cu clusters on the stoichiometric TiO_2(110) rutile surface, as depicted in Fig. 3

	A	B	C	D
Cu_2	3.07	2.57	2.54	2.27
Cu_3	3.61	3.30	3.11	1.63
Cu_4	3.69	3.30	–	–

the Ag and Cu clusters to the substrate, leaving the supported clusters positively charged. However the base of the supported Ag/Cu trimer is significantly stretched, which is we believe due to the strong ionic interaction between the positively charged base Ag and Cu atoms and the negatively charged O(2c) surface atoms.

We determine two stable structures for supported Ag and Cu tetramers [(4-A) and (4-B) in Figs. 3 and 4]. For both configurations, we initially placed a 2D rhombic structure with D_{2h} symmetry (which is the ground state of a neutral gas-phase Ag_4/Cu_4 cluster [21,22]) in between O(2c) rows and atop the O(2c) row, respectively. However, upon geometry optimization the 2D rhombic structure transforms into a 3D pyramidal structure. This appears to be consistent with experimental observations that the early stage growth (< 0.5 ML) of Ag and Cu clusters shows 3D like [11,24] mode while Au clusters are 2D like [12].

4. Summary

We present structural models for small Au_n, Ag_n, and Cu_n clusters ($n=2-4$) on rutile $TiO_2(110)$ and their relative stability based on planewave basis pseudopotential total energy calculations. We examine Au clusters on the reduced surface and Ag and Cu clusters on the stoichiometric surface. Our results show that the structure of these supported small clusters is determined by a combination of (i) particle ionization by charge transfer from the substrate, (ii) particle–substrate bonding interaction, and (iii) geometric constraint by the surface configuration of the support.

Acknowledgements

The authors acknowledge the Welch Foundation (Grant no. F-1535) for their financial support of this work. All our calculations were performed using supercomputers in Texas Advanced Computing Center at the University of Texas at Austin.

References

[1] A.T. Bell, Science 299 (2003) 1688–1691.
[2] A.K. Santra, D.W. Goodman, J. Phys. Cond. Matter 15 (2003) R31–R62.
[3] M. Haruta, Catal. Today 36 (1997) 153–166.
[4] M. Valden, X. Lai, D.W. Goodman, Science 281 (1998) 1647–1650.
[5] T.V. Choudhary, D.W. Goodman, Topics Catal. 21 (2002) 25–34.
[6] C.T. Campbell, S.C. Parker, D.E. Starr, Science 298 (2002) 811–814.
[7] A. Vijay, G. Mills, H. Metiu, J. Chem. Phys. 118 (2003) 6536–6551.
[8] D. Pillay, Y. Wang, G.S. Hwang, Korean J. Chem. Eng. 21 (2004) 537–547.
[9] F. Boccuzzi, A. Chiorino, M. Manzoli, D. Andreeva, T. Tabakova, L. Ilieva, V. Iadakiev, Catal. Today 75 (2002) 169–175.
[10] J. Zhou, D.A. Chen, Surf. Sci. 527 (2003) 183–197.
[11] D.A. Chen, M.C. Bartelt, S.M. Seutter, K.F. McCarty, Surf. Sci. 464 (2000) L708–L714.
[12] F. Cosandey, T.E. Madey, Surf. Rev. Lett. 8 (2001) 73–93.
[13] J.P. Perdew, J.A. Chevary, S.H. Vosko, K.A. Jackson, M.R. Pederson, D.J. Singh, C. Fiolhais, Phys. Rev. B 46 (1992) 6671–6687.
[14] D. Vanderbilt, Phys. Rev. B 41 (1990) 7892–7895.
[15] G. Kresse, J. Hafner, Phys. Rev. B 47 (1993) 558–561.
[16] Y. Wang, D. Pillay, G.S. Hwang, Phys. Rev. B 70 (2004) 193410.
[17] H. Hakkinen, U. Landman, Phys. Rev. B 62 (2000) R2287–R2290.
[18] X. Wu, L. Senapati, S.K. Nayak, A. Selloni, M. Hajaligol, J. Chem. Phys. B 72 (2005) 205422.
[19] D. Pillay, G.S. Hwang, Phys. Rev. B 72 (2005) 205422.
[20] V. Bonacic-Koutecky, J. Burda, R. Mitric, M.F. Ge, G. Zampella, P. Fantucci, J. Chem. Phys. 117 (2002) 3120–3131.
[21] P. Calaminici, A.M. Koster, N. Russo, D.R. Salahub, J. Chem. Phys. 105 (1996) 9546–9556.
[22] V. Bonacic-Koutecky, L. Cespiva, P. Fantucci, J. Koutecky, J. Chem. Phys. 98 (1993) 7981–7994.
[23] V. Bonacic-Koutecky, L. Cespiva, P. Fantucci, J. Pittner, J. Koutecky, J. Chem. Phys. 100 (1994) 490–506.
[24] K. Luo, T.P. St Clair, X. Lai, D.W. Goodman, J. Phys. Chem. B 104 (2000) 3050–3057.